2950 Niles Road, St. Joseph, MI 49085-9659, USA
269.429.0300 fax 269.429.3852 hq@asabe.org www.asabe.org

An ASABE Meeting Presentation

Paper Number: 083811

Surface Characteristics and Flowability of Distillers Dried Grains with Solubles

Rumela Bhadra, ASABE Member

Graduate Research Assistant, South Dakota State University, Brookings, SD 57007

Kurt A. Rosentrater, ASABE Member Engineer

Bioprocess Engineer, USDA, ARS, North Central Agricultural Research Laboratory, Brookings, SD 57006

K. Muthukumarappan, ASABE Member Engineer

Professor, South Dakota State University, Brookings, SD 57007

Written for presentation at the
2008 ASABE Annual International Meeting
Sponsored by ASABE
Rhode Island Convention Center
Providence, Rhode Island
June 29 – July 2, 2008

Abstract. With an annual production of approximately 6.5 billion gallons of fuel ethanol, and projected growth for the foreseeable future, supplies of coproducts such distillers dried grain with solubles (DDGS) are anticipated to continue to grow as well. DDGS is used primarily as livestock feed. Much of the DDGS must be shipped, often over large distances throughout the country, as much of the livestock (especially large dairies and feedlots) are outside the Corn Belt, where most of the ethanol plants are currently located. “Caking”, or stickiness, among particles is an important issue related to DDGS, especially when it leads to flowability problems when it is stored and shipped, this problem needs to be alleviated. Towards that end, the objective of this study was to understand the surface nature and characteristics of DDGS particles. The study examined the distribution patterns of chemical components of DDGS particles using standard staining biological techniques and stereo light microscopy. Surface chemical composition was also studied using confocal laser microscopy. Cross sectional staining of DDGS particles indicated a higher amount of protein thickness versus carbohydrate thickness in surface layers from DDGS that had lower flow function index, and thus greater cohesiveness, which indicates possible flow problems. Additionally, surface fat staining suggests that higher surface fat also occurred in samples with worse flow problems.

Keywords. DDGS, Flowability, Staining, Surface characteristics

Introduction

Distillers dried grain with solubles (DDGS) is one of the key co-products of a typical corn based dry milling bioethanol production plant. It has been estimated that approximately 85% of all energy consumed in USA is from fossil fuel sources (USDOE, 2007); this is expected to rise to meet enormous energy demands. Fossil fuel consumption will be dominated by China and India in future years due to exponential growth in population and expanding economies. As fossils fuels are nonrenewable and their supply will eventually diminish, it is very important to find renewable and greener sources of energy. Thus, there has been a tremendous potential and need for growth in the bioethanol industry in the past decade, and it is anticipated to increase in future years.

Corn is a predominant cash crop in the Midwest region of US, and is widely used to produce bioethanol for motor fuels. An exponential increase in the corn based ethanol industry, and thus DDGS, has occurred over the last several years. Every bushel of corn (56 lbs) yields about approximately 17 lbs of DDGS and 17.6 lbs of ethanol, along with a similar quantity of carbon dioxide (Jacques et al., 2003). It is forecasted that there was nearly 15 million tons of DDGS production by the end of 2007 in the US due to the contributions of newly constructed ethanol plants (AAFC, 2007); this level is anticipated to be even more in coming years. To maintain sustainability and viability in the ethanol industry, it is important to augment and increase the use of DDGS in both international and national domains, as only a portion of DDGS is being used currently in the Midwest (NASS, 2007), where the ethanol plants are located. DDGS mainly consists of non-fermentable sugars, protein, fibers, minerals, water–soluble vitamins, and amino acids. Due to its high energy content, DDGS is used extensively as livestock feed for ruminants and non-ruminants. DDGS typically contains about 86% to 93% (db) dry matter, 26% to 34% (db) crude protein, and 3% to 13% (db) fat (Rosentrater and Muthukumarappan, 2006). However, fat percentages are most often in the range of 8 to 12%.

DDGS is mainly transported through rail cars throughout the country after it is produced in the “Corn Belt” region of the mid US. Shipping, handling and storage of DDGS thus become crucial, because it often tends to have flowability problems, which may be due to various environmental factors. “Caking”, or hardening and agglomeration of DDGS particles, forms bridges among the particles and thus restricts the flowability of DDGS during unloading from rail cars. Flow problems may be caused by a number of factors, including excessive moisture content, fat levels, temperatures, humidity, etc. But there is currently a lack of complete information on these factors. Often these “cakes” must be broken by using a sledge hammer on the outside of the car, and thus US rail services have regulations regarding rails cars for DDGS shipping, due to potential damage to the cars during unloading at the delivery site.

There is a substantial amount of anecdotal knowledge about DDGS flowability from various sources, but there is a lack of complete understanding of the process (Rosentrater and Giglio, 2005; Rosentrater 2006a, b). In one study, DDGS was modeled using exploratory data analysis techniques to investigate data obtained from experimental measurements. This study was able to predict a simple and robust model (R^2=0.93, SE=0.12) by combining important flow properties obtained from conventional Carr (1965) and Jenike (1964) tests using response surface modeling and dimensional analysis (Ganesan et al., 2007a). However, that particular study was performed on DDGS samples from a single commercial plant. The DDGS samples used in that study were prepared on a laboratory scale, using mixtures of DDG and CDS at various levels. Thus, much more work is needed to further modeling studies related to DDGS flowability.

Flowability problems in DDGS may arise from the synergistic effects of environmental factors like humidity and temperature changes), time, compaction, pressure distribution throughout the product mass, chemical components (such as fat and sugar content), and other inherent

material properties (particle size, roughness, shape) and /or variations in the levels of above listed factors (Craik and Miller, 1958; Fitzpatrick et al., 2004a, b; Johanson, 1978; Moreya and Peleg, 1981; Teunou et al., 1999). Researchers have also worked with using flow agent $CaCo_3$ in DDGS in order to minimize flow restrictions due to caking of particles (Ganesan et al., 2006). Apart from DDGS, studies with flow agents like calcium stearate, aluminum silicate, and sodium dodecyl sulfonate have been studied for improving the flow properties in powders such as sucrose, lactose, modified starch and granular solids like ammonium percolate (Chen & Chou, 1993; Onwulata et al., 1996), and have been shown to be somewhat successful.

In depth analysis on the factors influencing DDGS flowability is essential. Some key factors which may be primarily responsible for the flowability problems in DDGS include moisture content, humidity, temperature variations, pressure, fat, and particle size and shape. Free fat content on DDGS surfaces is expected to play a vital role in granular flowability, but this aspect has not been studied thoroughly in DDGS, or in other variants of distiller's grain.

Previous work related to humidity and temperature in terms of DDGS flowability has examined the dynamic water absorption characteristics of DDGS using four soluble levels (10, 15, 20, and 25% db), at four temperatures levels (10, 20, 30, and 40°C) with four relative humidity levels (60, 70, 80, and 90%). This study was able to develop a comprehensive adsorption model termed the GRM model (R^2=0.94 and F=16503.90), which was based on soluble levels, relative humidity, and temperature effects, along with time and moisture content. Such a model is beneficial in predicting the dynamic adsorption characteristics of water in to DDGS for different storage conditions (Ganesan et al., 2007c). In an another study by the same authors, they were able to predict the sorption isotherm behavior of DDGS, again with varying soluble levels (10, 15, 20, and 25% db) and relative humidity levels (60, 70, 80, and 90%) and then determine the equilibrium moisture content (EMC). This study observed that the modified Halsey and modified Exponential models performed well for the isotherm data; however, another empirical model, termed the GMR model (R^2=0.94; F=977.55) was the best fit for the DDGS (Ganesan et al., 2007d).

Some work has been done on lowering the fat content of DDGS by removing the corn oil, which may improve the marketability of DDGS by increasing the total protein content. Moreover corn oil from DDGS can be used as a substrate for biodiesel (GS Agrifuels, 2006). Use of corn oil for biodiesel production can provide more diversity in the corn processing industry, but on the other hand, removing oil/fat from DDGS will alter the chemical and nutritional properties, and may also affect physical and flowability properties as well. High oil and low DDGS samples have been studied for flowability properties through Carr (1965) and Jenike Shear (1964), testing, and has shown that reduced fat showed somewhat less flowability problems (Ganesan et al., 2007b). However, it should be noted that the reduction of fat in these DDGS samples were done through solvent extraction and such reduction takes place from within and on the surface of particles. Studying the surface fat and other chemical compounds distributions, may be an interesting opportunity to examine the potential for flowability problems. A discussion of relevant techniques is thus warranted.

Microscopic Techniques for Food and Biological Particles

Beyond water interaction, chemical composition may also play a key role. For example, the distribution of fat in milk powders has a significant effect on functional properties such as wetability and dispersibility (Pisecky, 1997).Studies indicated a high fat content (about 20%) in spray dried milk produced worse flow in the resulting milk powder (Perez and Flores, 1997). Confocal scanning laser microscopy (CLSM) revealed that spray dried whole milk protein had very little surface fat compared to high fat free cream powder and roller dried milk powder; high fat free cream powder and roller dried milk powder had high levels of surface fat occluded within the particle and on the

inner lining of occluded air bubbles (Auty et al., 2001). Such difference in the distribution of fat within the particles, or on the surface of particles, can play a vital role in understanding flow problems related to such powders. Microscopic visualization of surface fat, fat globules, and coalesced fat has been studied extensively with the help of labeling selective fluorescent probes in milk powders (McKenna, 1997). Confocal laser microscopy has been able to reveal agglomerated regions of surface fat on milk powders which were likely to affect flow properties and solubility features (Buma, 1968 & 1971). Studies were also done in milk powders to estimate the effects of surface phospholipids localizations. It has been found out that storage of milk powders at lower temperatures reduces the amount of surface phospholipids that are available to act as amphiphillic wetting agents. Storage at such temperatures can reduce the amount of liquid fat, thus reducing mobility and improving wetability, thus reducing potential flow problems (McKenna, 1997). Such surface phospholipids estimation, localization, and other kinds of research based on this approach have been being done by using of fluorescently labeled phophatidylcholine probes with rhodamine filter block at 568 nm (McKenna, 1997).

Examination of relatively large particles like milk and chocolate powders requires use of a modern form of light microscopy known as confocal laser scanning microscopy (CLSM). The problem which arises with ordinary light microscopy is in focusing of such kind of larger particles. Observing milk powder particles with light microscopy will produce a blurred image due to large depth of focus, but can be handled by the usage of confocal laser microscopy (McKenna, 1997). In confocal laser scanning microscopy the image formation does not depend on transmitting light through the specimen. In confocal microscopy, a scanning laser illuminates a layer within the specimen at a specific focal plane and removes out of focus information by use of a pin hole, thus providing images with better resolution than the ordinary light microscopy (Heertje et al., 1987; Brooker 1991, 1995). The image from the confocal microscope is stored directly on computer and also images at each stages/plane can be seen moving the slide stage up and down, this helps the microscopist to see the internal three dimensional structure of the image. Special software is used to add these individual sections and produce a single image with higher clarity. Additionally, the individual images can be rotated to produce a three dimensional view of the object and easily can be communicated to nonmicroscopist (Gaonkar and McPherson, 2006). This technique is limited to particles with about 100 μm depth; this depends on the depth that the laser can penetrate. This technique is also limited by the laser wavelengths available and stains/dyes used for food or biological products (Gaonkar and McPherson, 2006). The images of components of food or any other biological particles like protein, fat, or lipids are produced by introducing a fluorescent dye to the food particles and then excitation of such dye with the help of laser at a selective wavelength.

Modern confocal laser microscopy contains combined krypton–argon lasers that can produce light at 488, 568, and 614 nm, which allow multiple fluorescent dyes to be excited. Thus, samples with dual labeled dye for protein and fat can be viewed simultaneously by the usage of such laser techniques (Brooker, 1995). In some studies, polarized light was used to follow the starch gelatinization properties, and found that starch gelatinization was linked to final dough development and final product quality (Seetharaman et al., 2004).

To distinguish individual nutritional components and their part in nature of the food requires the use of stains or dyes to highlight particular constituents. Most stains are general rather than specific, but are useful for indentifying ingredients such as proteins, starch, polysaccharides, and fat (Gaonkar and McPherson, 2006). Commonly used stains are iodine in potassium iodide for starch to indicate the amylase chains in blue-black or amylopectin in red-brown color (Gaonkar and McPherson, 2006). Light green, eosin, or toluidine blue is commonly used for staining proteins although iodine can also stain protein yellow. Toluidine blue is known as metachromatic stain, which means it will stain different colors depending on the ionic environment and nature of the

material. It can distinguish between polysaccharides (pink color) and proteins (blue-green) if it is applied with precise concentrations and carefully (Gaonkar and McPherson, 2006).

Fats are typically stained slowly with either a Sudan series stain or Nile blue. Standard protocols for fat staining like oil red, oil propylene glycol, osmonium tetraoxide method for fat frozen sections (Mallory, 1961), Landings method of lipid staining by aqueous eosin solution for both paraffin and frozen sections (Landing et al., 1952), Pearse's method of detection of phospholipids by neutral red solutions (Pearse, 1955) and many more sophisticated techniques are available. The advantage to using different stains for each ingredient is that it helps to distinguish and see the interactions between ingredients (Gaonkar and McPherson, 2006).

Plant cells as well as animal cells have been studied extensively using fluorescence. An interesting review of identification of components in cereals has been provided by Fulcher (1982). Nutritional components in chocolate powders and its interaction on the effect of food's physical properties like melting and flowability has been studied extensively using confocal laser microscopy (Subramaniam et al., 1994); protein and sugar interactions, study of protein network, effect in lower melting temperatures, and restrictions in fat molecules have been observed in the above study. Loren et al. (1999) combined confocal laser scanning microscopy with image analysis to determine the microstructure of gelatin–maltodextrin systems to understand and asses the boundary interactions or interfacial areas. In another study, confocal laser scanning microscopy was used to determine the interaction between an emulsifier and beta – lactoglobulin during gelation. They presented dynamic studies of formation of gels with and without emulsifier (Hermansson et al., 2000).

Dyes or stains play an important role in determining the success of the experimental procedure and accuracy of the images. All dyes are generally benzene derivative compounds, replacing two hydrogen atoms in the benzene ring with oxygen atoms or with another atom or group having two valency bonds instead of one, which results in a readjustment of double bonds and the formation of a colored compound (Carson, 1926). A group that confers the property of color is called chromophore. The fundamental groups involved are C=C, C=O, C=S, C=N, N=N, N=O, and NO_2; the more these groups occurs in the compounds the more pronounced the color is (Carson, 1926). Although a compound having chromophore can act as a dye, it is essential that it should have the ability to bind to any tissue or biological material. Such ionizing groups in the chromophores are called auxochrome which enables the dye to link firmly to the tissue. The fundamental basic auxochrome groups is amino groups ($-NH_2$) and usual acidic auxochrome group is sulfonic acid ($-SO_3$), carboxyl groups (-COOH) and Hydroxyl groups (-OH) (Carson, 1926). pH of the solution, temperature changes, presence of salts, and concentration of dye molecules are some of the key factors that affect the binding capacity of the dye to food or tissue matrix.

Hematoxylin and Eosin (H&E) Staining

Hematoxylin and Eosin staining is mainly used for staining animal tissue for proteins and nuclei. Hematoxylin is extracted from logwood of the *Haematoxylon campechianun* tree, which is extensively grown in Jamaica. Freshly cut wood, when exposed to atmospheric conditions, turns brownish-red giving the oxidation product of hematoxylin known as hematein, which forms a weak anionic dye and binds essentially with nucleus content of the tissue. Harris Hematoxylin (Harris, 1900), Delafield hematoxylin (Delafield, 1885), Ehrlich hematoxylin (Ehrlich, 1886), and Weigert Hematoxylin (Weigert, 1904) are some common hematoxylin dye solutions used in tissue staining. Each of the hematoxylin dye solution preparations varies in the amount of hematoxylin as well as content of other supporting solutions like mordant, solvents, etc. For detailed descriptions and formulation of each hematoxylin dye, refer to Bancroft and Gamble (2002).

Plasma stains like eosin are most frequently anionic, or negatively charged dyes that combine with very cationic, or positively charged, tissue groups like the basic amino acids. Amino groups like arginine, histidine, and lysine are common binding sites for eosin dye. Eosin is fully charged at a pH of 7, but because the isoelectric point (IEP) of most protein is approximately 6, we must stain below pH 6 to develop a net positive charge on protein and facilitate binding with eosin dye instead of precipitation (Carson, 1926). Below pH 4, the eosin will nonspecifically bind to sections due the conversion of eosin in free acid at that low pH. Hence, the best pH for eosin dye is 4.6 to 5. Two common types of eosin solutions used in tissue staining are Eosin Y and Eosin B; the detailed formulation and concentration of such eosin preparation can be found in Carson (1926). In animal tissue it is commonly used to stain erythrocytes, collagen and cytoplasm of muscle or epithelial cells. Eosin imparts typically pink shades to the tissue or cells in presence of such amino acids and thus estimating protein content, while the counter stain hematoxylin imparts blue color indicating presence of nucleus.

Periodic Acid Schiff (PAS) Staining

Carbohydrates are important organic compounds that include sugars, starch, cellulose and polymers that are mostly linked to protein. Carbohydrates are defined chemically as ketone or aldehyde derivatives of polyhydroxyl alcohols, and are classified broadly as monosaccharide (with one sugar unit), oligosaccharides (ten to twelve sugar units) and polysaccharides (with many sugar units) (Das, 1992). Glucose is the only monosaccharide found in biological cells or substances. Neutral polysaccharides such as glycogen, starch, cellulose, and chitin give very positive reaction with PAS staining. Apart from the above typical polysaccharides, it also can impart color to glycoproteins and glycolipids (Carson, 1926). In animal tissues it is mainly used as the indicator for glycogen content in basement membranes and liver tissues (Bancroft and Gamble, 2002). This is because glycogen is the major polysaccharide present in the animal tissues. The principle of this reaction with carbohydrates is in the oxidative cleavage of the carbon–to-carbon bond in 1, 2 glycols or their amino or alkylamino derivatives to form dialdehydes. These aldehydes will react with fuschin-sulfurous acid present in Schiff reagent which combines with basic pararosaniline to form magenta–colored compound, which is imparted to carbohydrate-rich tissues or cells (Stoward, 1967).

There is no documented study on the surface composition or characteristics of DDGS particles, or their possible cause in flowability problems. “Caking” (or bridging) phenomena between two particles are most probably a surface process, which thus impacts the characteristics of the whole DDGS mass. Thus, the objective of this study was to evaluate the surface properties of DDGS in terms of chemical components (protein and fat) and to investigate their role in the flowability of DDGS.

Materials and Methods

Sample Collection

Samples of DDGS were obtained from five commercial ethanol plants across the state of South Dakota, in two collection periods. The samples were stored in Ziploc plastic bags under normal room temperature (24 ±1°C) and humidity conditions. The DDGS samples were then segregated based on their particle size using a Rotap Sieve analyzer (model RX-29, Mentor, OH) using 4 US standard sieve sizes (2.38 mm, 1.68 mm, 1.19 mm, 0.84 mm diameter). Particles from each sieve were collected and used for both cross sectional staining of protein and carbohydrate content, and then for surface staining for fat content.. For H& E (protein) and PAS (carbohydrate) staining, three replications were performed for each particle size from each plant, each batch. Thus, we had 3×4×5×2 =120 samples for PAS and H&E staining respectively. For fat staining, one

replication was used for each of the five plants, for 5×2=10 samples for only one sieve size (0.074 mm diameter).

Proximate Analysis and Physical Properties

Protein content was determined using method 990.03 (AOAC, 2003), and fat content with method 920.39 (AOAC, 2003); total starch was measured following Xiong et al. (1990). Ash content was determined using method 08 – 01 (AACC, 2000). Acid Detergent Fiber (ADF), Neutral Detergent Fiber (NDF), and crude fiber analysis was done with an ANKOM fiber analyzer (Model 200 ANKOM Technology, Macedon, NY).

The soluble content of the DDGS samples were determined using the technique developed by Ganesan et al. (2006a). The moisture content of each sample was determined using AACC method 44-19 (2000), by the use of a forced convection laboratory oven (Thelco Precision, Jovan Inc. Wincester, VA). The geometric mean diameter and geometric standard deviation of DDGS particles were calculated using ASAE/ANSI standard S319.3 (2004), and the segregation of the particles was accomplished using a Rotap sieve analyzer (Mentor, OH).

Cross-Sectional Staining of DDGS Particles for Carbohydrate and Protein

DDGS particles collected from US sieve no. 8 (2.28 mm diameter), 12 (1.68 mm diameter), 16 (1.19 mm diameter), and 20 (0.841 mm diameter) were packed in a microcassette which was soaked overnight in an automatic tissue processing unit (Shandon Excelsior R 13506 Thermoelectron, Pittsburgh, PA). After overnight processing the DDGS particles were embedded in paraffin solution and cooled subsequently to hold the particles and for sectioning in later stages. Fine sections of about 5 mm thick film were cut using a microtome tissue cutter (Leica RM 2125, North Central Instrument, Plymouth, MN) and then placed on positively charged glass micro slides.

After preparing the fine cross sections of DDGS particles, they were then put in Shandon Varistain 24-4 (Cheshire, UK) for automated H & E staining (protein). The processing procedures were performed at the Histology section of the Veterinary Science Department, Animal Disease Research and Diagnostic Laboratory (ADRL), South Dakota State University.

For PAS staining (carbohydrate), each of the above DDGS particles was deparafinized using Shandon Varistain 24-4 (Cheshire, UK), and then the following sequential steps were carried out:

1. Section slides were placed in 1% periodic acid for 10 min.
2. The above slides were washed well in running tap water for 10 min
3. Slides were rinsed well in distilled water
4. Slides were placed in Schiff's reagent for 15 min
5. Slides were placed under running tap water for 10 min
6. Slides were counterstained with light green for 20 sec
7. Slides were dipped in 95% ethyl alcohol for 40 sec and then in formula 83 for another 40 sec
8. Each of the micro slides were dried, and then mounted using Anantech mounting media

Formula 83 is a specially prepared solution. PAS staining was also performed at the Histology section of Veterinary Science Department, Animal Disease Research and Diagnostic Laboratory (ADRL), South Dakota State University. Each of the stained sections of DDGS from specified sieve sizes were observed under an Olympus SZ 10 stereomicroscope with DP digital camera at the Genomic Core Facility laboratory of South Dakota State University. Each of the

images of DDGS cross sections were then analyzed using ImageJ (version 1.38x) software (Rasband, 1997-2007).

Surface Fat Staining of DDGS Particles

The fat labeling for DDGS particles from US Sieve no. 200 (0.074 mm diameter) was performed using a fluorescent probe (Sigma Aldrich Nile Red, Saint Louis, MO) and 1,2 propanediol solvent (Sigma Aldrich Saint Louis, MO) at the concentration of 0.02 g/L as discussed in Auty et al. (2001). Nile red, or formally known as Nile Blue A oxazone dye, diffuses readily into the lipid or fat phase, and becomes strongly fluorescent when excited in the range of 450 – 500 nm (McKenna, 1997). In order to reduce nonspecific interaction and trapping of the fluorescent dye in between the DDGS particles, it was washed with 1,2 propanediol solvent (Sigma Aldrich, St. Louis, MO) and centrifuged at 10000 rpm for 10 min. This procedure was carried out for three times for each sample, using a Sorvall Legend ^{TM} RT centrifuge (ThermoElectron Inc., Asheville, NC). This was done to reduce spurious or extra fluorescence from the samples, and led to more accurate observations. Each time the supernatants were removed, and specifically stained, fine DDGS particles were collected from the residue. The DDGS samples were then excited at a wavelength of 488 nm using a fluorescein isothiocyanate block filter of an Olympus Fluroview FV 300 Laser Scanning Confocal Microscope System interface with an IX 81 microscope (Leeds Precision Instruments, Minneapolis, MN). This procedure was performed at the Genomic Core Facility at South Dakota State University.

Statistical Analysis

For each property, formal statistical data analysis were done using Microsoft Excel v.2003 (Microsoft Corp., Redmond, WA); Least significant Test (LSD) at 95% confidence level was performed with SAS software (SAS Institute, Carry, NC). The LSD test on the carbohydrate and protein were performed to determine if there were differences between the plants across all batches, and between the batches of each single plant.

Results and Discussion

Proximate Analysis and Physical Properties

Table 1 presents the proximate analysis of the DDGS samples used in this study. The crude protein was from 28.33 to 30.65% db, and neutral detergent fiber (NDF) was found to be from 31.84 to 39.90 % db. These two chemical constituents were highest in terms of content in DDGS, followed by acid detergent fiber (ADF), total starch, ash, crude fat, and crude fiber. The composition of protein and fiber contents determined by proximate analysis and by the cross-sectional staining procedure, were actually very close. Table 2 and table 3 gives the protein and carbohydrate compositions measure through microscopy. From table 3 we can see that the overall carbohydrate composition was found to be from 29.88 % (db) to 31.90% (db) and protein composition was from 24.56% (db) to 30.47% (db). Some differences were observed in terms of content between the two procedures. Cross-sectional staining was done for each of the sieve sizes, and then protein and carbohydrate content were determined using software analysis, but for proximate analysis composition was determined for whole DDGS particles, and no separation of particles were done according to sieve sizes; this might be the reason for the slight differences in the protein and carbohydrate content between the staining and proximate analysis.

Table 2 gives the results of the composition of carbohydrate and protein content in DDGS particles for their respective screen sizes (diameters) as mentioned above, after analysis of cross sectional staining images through ImageJ software. We can clearly observe the two most important features of this analysis: first, there are no fixed zones where protein and carbohydrates

resided separately across the cross section of each particle. This shows the very probable possibility of finding protein and carbohydrates intermingled together in the DDGS particles with various covalent and non-covalent interactions between protein and carbohydrate molecules; Secondly, there was no definitive trend in the composition amongst particle size for a particular sample type. For example, plant 3, batch 2 DDGS particles from sieve no. 20 (0.841 mm diameter) had about 26.50% of protein, while the same sample showed only 16.50% protein for particles at sieve no. 8 (2.38 mm diameter). These differences in the nutritional compositions between sieve sizes were quite similar to results stated in Ileleji et al. (2005). This shows that a change in the particle size (from different sizes) may change nutritional components. However, in plant 4, batch 1 and in plant 2, batch 1 we observed a very narrow range of carbohydrate percentages among the sieve sizes; 22.84 to 29.45% and 24.60 to 28.15%. Figure 1 represents the DDGS samples with cross sectional staining images for carbohydrate and protein content.

Table 3 presents the average protein and carbohydrate content determined for each sieve size through cross-section staining of DDGS particles. Plant 1 shows a higher carbohydrate content (39.59 to 46.96 %) compared to the other plants. Plant 5 had higher protein content (25.13 to 33.86%) compared to the other plants, but plant 1 (19.57 to 40.39%) had more broad range for protein content. The highest carbohydrate content of 43.06% was found in the sieve size 8 (2.32 mm) (plant 1) and highest protein content (40.39%) was found in sieve size 12 (1.68 mm) (plant 1).

Table 4 presents some physical and particle properties for the DDGS used in this study. Moisture content for all sample types was found below 9% db, and soluble level was found between 11.26% to 14.80% db. The highest geometric mean diameter was found for plant 3, with a mean value of 1.19 mm.

Table 5 presents some flowability parameters that were reported in our previous study which was based on the same commercial DDGS samples (Bhadra et al., 2007). For plant 1, batch 1 we observed a higher amount of carbohydrate than protein (table 2), and we can clearly observe there were less flow problems due to lower angle of repose value (35.95°) and higher Jenike flow function index (4.56). According to Carr classification of flowability (Carr, 1965), the higher the angle of repose (> 45°) the higher is the flow problem; particles having angle of repose between 36° to 40° should have fairly good flow. A Jenike flow function higher than 4 would indicate a reasonably good flow, while a flow function value less than 4 would suggest a cohesive solid, according to standard Jenike flow classifications (Jenike, 1964). The flow function index is given as:

$$F = \sigma_1 / \sigma_c \quad (1)$$

where σ_1 is defined as the major consolidation stress, and σ_c is unconfined yield stress which measures the major compressive strength in the material during flow. Classification of flowability of powders, based on the flow function index, is given in table 7. Thus, for plant 1, batch 1 there was fairly good flow behavior (intermittent flow). Total flowability index for all plants and batches were from 79.20 to 82.40 which according to Carr classification indicates good flow (Carr, 1965). But on the other hand the floodability index was higher than normal levels, which indicated that there may be potential flushing of DDGS materials, that is the particles may tend to flow abruptly and sporadically, which can deteriorate the quality of flow and is not desired. Since the Jenike (1964) procedure is close to actual industrial situation, it may be more logical to relate the results of carbohydrate and protein compositions with the Jenike flow function indices.

From Table 2 and 5, in plant 3, batch 1 we obtained higher percentages of carbohydrates (ranges from 22.64 to 40.85%) than protein (ranges from 23.28 to 27.51%), and higher values of Jenike flow function index at Level 1 consolidation (5.57) and Level 2 consolidation (5.69), which indicates good flow. Plant 5, batch 2 (table 2 and 5) had higher amount of protein percentages (minimum value of 27.14%) than carbohydrates (minimum value 21.46 %), in the DDGS particles

and they also showed relatively lower value of flow function indices for both consolidation levels (3.07 for Level 1 and 1.90 for Level 2), suggesting potential flow problems. Again, we observed that for plant 5, batch 1 the protein and carbohydrate composition was very close, and it also had low flow function of 3.28 and 2.18 for Level 1 and Level 2 consolidation, respectively (table 5). Such low values of flow function indices indicate cohesive flow, according to the Jenike classification. This indicates that there is logical reasoning between percentages of carbohydrate and protein with flowability in DDGS.

A higher amount of protein could possibly lead to protein-protein or protein-ligand interactions. For Example, driving forces involved in intra-molecular interactions are also the driving inter-molecular interactions, and can be a cause of worse flow problems in whey protein concentrates, milk and chocolate powders (Gaonkar and McPherson, 2006). During changes in environmental conditions, like high temperatures, changes in salt concentration, or more water molecules, protein can change its conformations and as a consequence reactive amino acids which were buried inside the core of DDGS particles may surface to form possible interactions which may lead to caking or bridging between particles (Gaonkar and McPherson, 2006). At very short distances, van der Waals forces can drive proteins to interact. Presence of charged/polar amino acids may form Ca^{2+} bridging, which is commonly known as salt bridges in proteins. In has been found, for example, that in whey protein powder there was stability of α lactalbumin protein when there was an increase in Ca^{2+} (Boye et. al., 1997). DDGS is found to have charged amino acids residues like histidine, lysine, threonine, and arginine (Speihs et al., 2002), but DDGS from Minnesota and South Dakota was found to lower in Ca^{+2} content but higher in phosphorous levels (Speihs et al., 2002). Additionally, DDGS from Minnesota and South Dakota were found to have higher amounts of threonine (1.13%) and arginine (1.2%) content (Spiehs et al., 2002). Thus, formation of salt bridges with phosphorous or other salts may be possible for the amino acids residues in DDGS, and may lead to worse flow problems.

Aggregation in protein molecules can cause hardening in gels (Mulvihill et al., 1988). Hydrophobic interactions and electrostatic charge interactions during protein-protein or protein–ligand interactions plays a fundamental role in attraction of particles (Gaonkar and McPherson, 2006). Non polar amino acid residues such as valine, isoleucine, and leucine were in found in DDGS at levels of 1.5%, 1.12%, and 3.55%, respectively (Spiehs et al., 2002) . Such non polar amino acids are often buried in the core of DDGS particles due to hydrophobicity, but it can also change its surface hydrophobicity due to environmental conditions like heat (Nakai, 1983). On such an event, two DDGS particle with sufficient moisture film on it may interact with one another to remove the water molecules (hydrophobic effect) on their surface; thus in this process, they can form an aggregate particle, which can lead to flow restrictions on a larger scale.

Hausner Ratio is defined tapped (or packed) bulk density divided by aerated (or loose) bulk density. Hausner Ratios higher than 1.25 indicates bad flow in solid powders (Michael, 2001). Bulk density or Hausner ratio influences the functions and design parameters like arching, rat-holing, limiting flow rate from hopper and equipment structural design (Johanson, 1978). The samples of DDGS used in this study all had Hausner Ratios much lower than 1.25.

Cross-Sectional Carbohydrate and Protein

Table 6 indicates the surface thickness of carbohydrate and protein layers for DDGS particles, but only from sieve no. 8 (2.28 mm diameter) We observed that plant 3, batch 1 had the highest thickness for carbohydrate layer (4.80 μm) and also had the highest Jenike flow function indices (Table 5). Likewise for plant 4, batch 1 we obtained higher thickness for protein layer at the surface (3.21 μm) than carbohydrates, and this sample also had a lower flow function index, which means cohesiveness in DDGS. Higher flow function index (>4) typically indicates good flow in solid materials (Jenike, 1964). Presence of relatively higher amounts of protein on the surface than

carbohydrates will lower flow function index, which represents cohesive or bad flow, and can be logically understood in terms of protein-proteins interactions as explained above.

There was also the presence of the blue color counter stain in H & E stained particles, indicating the possibility of nucleus and nucleic acids. Since DDGS is formed as the coproduct of a fermentation process in industry with yeast microbes, it is probable that the yeast protein as well as nucleic acid material from yeast cells imparts blue color in H&E staining. Negative charges on DNA and nucleic acids from damaged corn and yeast cells can also facilitate electrostatic attraction between two DDGS particles, and could therefore lead to aggregation of DDGS particles and flow problems.

Ideally DDGS should have no starch in it, because during corn fermentation to ethanol, practically all the starch should be fermented to alcohol by yeast. However, from our previous study, we have obtained about 10% starch content (from 9.81% to 11.59%) indicating some inefficiency in the process (Bhadra et al., 2007a). This presence of starch molecules in DDGS was also depicted in the PAS staining of polysaccharides, and can be another reason for flow problems (i.e., starch gelatinization at higher temperatures). Starch gelatinization would bring about stickiness in DDGS, and would lead to flow problems.

Surface Fat

Figure 2 shows the presence of fat globules on the surface of DDGS surface particles upon the application of fluorescent probe. Each image was taken at 10 X magnification using confocal laser microscopy with a 1/5.6 sec exposure time. For plant 2 (batch 1), plant 1 (batch 2), plant 4 (batch 2), and plant 5 (batch 2) we observe fat globules of more than 10 μm and more concentration of fluorescence. This indicates a higher amount of surface fat on those particles. Regions of surface could be clearly observed and they appear to be agglomerated. Such observations in food powders have been found to be related to flow problems (Buma, 1968 & 1971). The scale bar used for all the images in figure 2 is 10 μm. From figure 2, for plant 2 (batch 1), plant 4 (batch 2), and plant 5 (batch 2) surface fat globules were more than 10 μm mostly from 20 μm to 40 μm. We can also observe higher concentrations of fat globules in them. From table 5 we can clearly see that the above stated DDGS samples had Jenike flow function indices 1.43, 3.27, and 3.07, respectively. These ranges of flow function index indicate cohesive flow in the DDGS, according to Jenike classification, which is shown in table 7. Thus, our observations indicated that fat could be a possible reason for flow problems in DDGS.

We can also observe that the fat globules in plant 1, batch1 were of less concentration, and this sample had a flow function index of 4.56, indicating good flow (Figure 2). We also observed that plant 1 (batch 2) had relatively larger surface fat globules, but showed high Jenike flow function index, which means it had good flow characteristics. Sometimes higher fat concentration appears to lubricate DDGS particles and facilitate good flow.

The relationship of higher amount of surface fat with poor flow is logical, as fat molecules on DDGS surfaces have been found to play an important role in flowability for other granular materials. Fat molecules at high temperatures may liquefy and act as glue between particles, thus leading to stickiness and caking. It has been found that fat produced worse flow problems in soy milk powders (Perez and Flores, 1997). However, plant 1 (batch 2) had the highest amount of fat droplets, but a flow function index of 5.35, indicating good flow. These kinds of results reveal that flowability is not only dependent on surface fat composition, but also on other chemical, physical, and environmental factors. Surface phospholipids estimation using specific fluorescent probes could also be done to estimates their role in agglomeration of DDGS particles.

Since DDGS is a biological particle, it is natural that there would be some auto fluorescence from the particle itself, even without specific fluorescent probes, when excited with

laser. Figure 3a represents the image of a control sample of DDGS particles at 10X magnification, using the same exposure time of the camera. There was some auto fluorescence observed, as shown in figure 3a, but definitely it was present in minor traces when compared to actual surface fat staining. Since these kind of microscopic staining research with DDGS particles has not been done before it is therefore not possible to compare these findings with previous studies.

Conclusions

Form the above discussion it was very evident that higher protein and fat levels in DDGS indicated worse flow problems which leaded to "caking" of particles. Not only fat but protein structure, its interaction, denaturation patterns can be substantially good reason for the DDGS particles to stick together. Microscopic and staining techniques combined with sophisticated image analysis software were able to predict more evidential and quantitative results to understand flowability problems in DDGS. Since flowability is multivariate problem it is therefore important to focus of various aspects of the DDGS particles. More future research is necessary in this area for a better understanding of flowability.

Acknowledgements

The authors would like to extend their sincere thanks to Dr. Tanya D. Graham, Dr. Frank Qin, Joel Zebill, Margaret Perry, and all the other staff members in the department of Veterinary Science; the Genomic Core Facility, and Dr. Michael Hildereth, South Dakota State University, who aided with the staining and microscopy work. We would also like to extent our sincere gratitude to all the ethanol plants who generously contributed DDGS samples for this research. We appreciate the financial support provided by Agricultural Experiment Station at South Dakota State University and USDA-ARS to complete this project.

References

AACC. 2000. Approved Methods, 10th ed. St. Paul, MN: American Association of Cereal Chemistry.

AOAC International. 2003. Official Methods of Analysis of the Association of Analytical Chemists, 17th Ed. Method 920.39. The Association: Gaithersburg, MA.

AAFC. 2007. Protein meal: Situation and outlook. Agriculture and Agri-Food Canada, Bi weekly Bulletin 19(3): 1-4.

ASAE. 2004. S19.3 Method of determining and expressing fineness of feed materials by sieving. *ASAE Standards*. St Joseph, MI: ASABE.

Auty, M. A. E., M. Twomey, T. P. Guinee, and D. M. Mulvihill. 2001. Development and application of confocal scanning laser microscopy methods for studying the distribution of fat and protein in selected dairy products. Journal of Dairy Research 68:417-427.

Bancroft, J.D. and M. Gamble. 2002. Theory and practice of histological techniques, 5th ed., , London, UK; Harcourt Publishers limited.

Bhadra, R., K. Muthukumarappan, and K. A. Rosentrater. 2007. Towards an understanding of DDGS flowability characteristics. CSBE/ASABE North central intersectional conference, Paper No: RRV07148. St. Joseph, MI. ASABE

Bhadra, R., K. Muthukumarappan, and K. A. Rosentrater. 2007a. Characterization of chemical and physical properties of distillers dried grain with solubles (DDGS). Annual International Meeting, Paper No: 077009. St. Joseph, MI: ASABE

Boye, I., I. Alli, and A. A. Ismail. 1997 Use of differential scanning calorimetry and infrared spectroscopy on the study of thermal and structural stability of α lactalbumin. Journal of Agricultural Food Chemistry 45:1116-1125.

Brooker, B. E. 1991. The study of food systems using confocal laser scanning microscopy. *Microscopy and Analysis* 27:13-15.

Brooker, B. E. 1995. Imaging food systems by confocal laser scanning microscopy. *In* New Physico–Chemical Techniques for the characterization of complex food systems. Pp. 533-68 (ed. E. Dickenson). London: Blackie Academic and Professional Publishers.

Buma, T. J. 1968. A correlation of free fat content and moisture content of whole milk spray powders. Netherlands Milk and Dairy Journal 22:22-28.

Buma, T. J. 1971. Free fat in spray–dried whole milk. Ph. D dissertation. Agricultural University, Wageningen, Netherlands.

Carr, Jr., R. L. 1965. Evaluating flow properties of solids. Chemical Engineering 72(3): 163-168.

Carson, F. L. 1926. Histotechnology–A Self Instruction Text, 2nd ed., (Chapter 6 & 7) Chicago. US. American Society of Clinical Pathologist Press.

Chen, Y. L. and J. Y. Chou. 1993. Selection of anticaking agents through crystallization. Powder Technology 77:1-6.

Craig, D. J. and B. F. Miller. 1958. The flow properties of powders under humid conditions. Journal of Pharmacy and Pharmacology 10:136-144.

Das, D. 1992. Biochemistry. 7th edition. Calcutta, India: Academic Publishers.

Delafield, J. cited by J. M. Prudden. 1885. Zeitschrift für wissenschaftliche Mikrosckopie und für mikroskopishe technik. 2:228.

Ehrlich, P. 1886. Fragekasten. Zeitschrift für wissenschaftliche Mikroskopie und für mikroskopiche Technik. 3: 150.

Fitzpatrick, J. J, S. A. Barringer, and T. Iqbal. 2004a. Flow property measurement of food powders and sensitivity of Jenike's hopper design methodology to measure values. Journal of Food Engineering 61(3):399-405.

Fitzpatrick, J. J, T. Iqbal, C. Delaney, T. Twomey, and M. K. Keogh. 2004b. Effect of powder properties and storage conditions on the flowability of milk powders with different fat contents. Journal of Food Engineering 64(4):435-444.

Fulcher, R. G. 1982. Fluorescence microscopy of cereals. Food Microstructure 1:167-175.

Ganesan V., K. A. Rosentrater, K. Muthukumarappan. 2006a. Methodology to determine soluble content in dry grind ethanol coproduct streams. Applied Engineering in Agriculture 22 (6): 899-903.

Ganesan V., K. A. Rosentrater, and K. Muthukumarappan. 2007a. Modeling the flow properties of distillers dried grains with solubles (DDGS). Cereal Chemistry 84(6):556-562.

Ganesan V., K. A. Rosentrater, and K. Muthukumarappan. 2007b. Physical and flow properties of regular and reduced fat distillers dried grains with solubles (DDGS). Food and Bioprocess Technology (in press) doi:10.1007/s11947-007-0026-x.

Ganesan V., K. A. Rosentrater, and K. Muthukumarappan. 2007c. Dynamic water adsorption characteristics of distillers dried grains with solubles. Cereal Chemistry 84(6):584-555.

Ganesan V., K. Muthukumarappan, and K. A. Rosentrater. 2007d. Sorption isotherm characteristics of distillers dried grain with solubles (DDGS). Transactions of ASABE (in press).

Ganesan, V., K. Muthukumarappan, and K. A. Rosentrater. 2006. Effect of flow agent addition on physical properties of DDG with varying moisture content and soluble percentages. ASABE annual meeting, Paper No: 066076. St Joseph, MI: ASABE.

Gaonkar, A. K. and A. McPherson (ed.). 2006.Chapter 2: Microscopy a tool to study ingredient interactions in food. Ingredient Interactions Effect on Food Quality, 2nd ed. Boca Raton, FL: CRC Taylor and Francis Group

GS Agrifuels. 2006. GS Agrifuels to convert corn oil into biodiesel to ethanol facilities. http://www.tmcnet.com/enews/e-newsletters/alternative-power/20061108/u2064140-gs-agrifuels-convert-corn-oil-into-biodiesel-ethanol.htm. Accessed on 15 January 2008

Harris, H. F. 1900. On the rapid conversion of hematoxylin into hematein in staining reactions. Journal of Applied Microscopic Laboratory Methods 3: 777.

Heertje, I., V. Der. Vlist, J. C. G. Blonk, H. A. C. Hendrickx, and G. J. Brackenhof. 1987. Confocal Scanning Laser microscopy in food research: some observations. Food Microstructure 6 115-120.

Hermansson, A.M., M. Langton, and N. Loren. 2000. New approaches to characterizing food microstructures. MRS Bulletin December: 30-36.

Ileleji, K. E., R. L. Stroshine, and K. S. Prakash. 2005 Segregation during gravity driven discharge of distiller's grain with solubles. ASASE Annual meeting Paper No: 066115. St. Joseph, MI: ASABE

Jaques, K. A., T. P. Lyons, and D. R. Kelsall. 2003. The Alcohol Textbook. Nottingham Nottingham. UK: University Press

Jenike, A. W. 1964. Storage and Flow of Solids. Bulletin No. 123. University of Utah: Utah Engineering Station.

Johanson, J. R. 1978. "Know your material-how to predict and use the properties of bulk solids". Chemical Engineering/Date Book Issue, October 30: 9-17.

Landing, B. H., L. L. Uzman, and A. Whipple. 1952. Lab Investigations 1:456-462.

Loren, N., M. Langton, and A.M. Hermansson. 1999. Confocal laser scanning microscopy and image analysis of kinetically trapped phase –separated gelatin/ maltodextrin gels. *Food Hydrocolloids* 13:185-198.

Mallory, F. B. 1961. Pathological Technique. p 118, New York, NY: Hafner Publishing Co.

Michael, A. E. 2001. Pharmaceutics: The Science of Dosage From Design, 2nd ed. London, UK: Churchill Livingstone.

McKenna, B. A. 1997. Examination of whole milk powder by confocal laser scanning microscopy. Journal of Dairy Research 64:423-432.

Moreyra, R., and M. Peleg. 1981. Effect of equilibrium water activity on the bulk properties of selected food powders. Journal of Food Science 46:1918-1922.

Mulvihill, D. M. and J. E. Kinsella. 1988. Gelation of β lactalbumin: effects of sodium chloride and calcium chloride on the rheological and structural properties of gels. Journal of food science 53:231-236.

Nakai, S. 1983. Structure function relationship of food protein with an emphasis on the importance of protein hydrophobicity. Journal of Agriculture Food Chemistry 31:676-683.

NASS. 2007. Ethanol coproducts used for livestock feed. Washington, D.C.: National Statistics Service, USDA. Available online: www.nass.usda.gov/Statistics_by_State/Iowa/Publications/Annual_Statistical_Bulletin/2007/07_111.pdf.

Onwulata C. I., R. P. Konstance, and V. H. Holsinger. 1996. Flow properties of encapsulated milk fat powders as affected by flow agent. Journal of food Science 61(6):1211-1215.

Pearse, A. G. E. 1955. Journal of Pathological Bacteria 70:554-557.

Perez, M. F. and R. A. Flores. 1997. Particle size of spray dried soymilk. Applied Engineering in Agriculture 13(5): 647-652.

Pisceky, J. 1997. Achieving product properties. *In Handbook of Milk Powder Manufacture*. pp. 149-191. Copenhagen. Denmark: Niro A/S

Rasband, W. S. 2007. ImageJ U.S. National Institute of Health, Bethesda, Maryland, USA; http://rsb.info.nih.gov/ij/.

Rosentrater, K. A. 2006a. Understanding distillers grain storage, handling and flowability challenges. Distillers Grains Quarterly 1(1):18-21.

Rosentrater, K. A. 2006b. Understanding flowability- part 2: Some key parameters. Distillers Grains Quarterly 1(2):20-23.

Rosentrater, K. A. and K. Muthukumarappan. 2006. Corn ethanol coproducts: Generation, properties, and future prospects. International Sugar Journal 108(1295):648-657.

Rosentrater, K. A. and M. Giglio. 2005. What are the challenges and opportunities for utilizing distillers grains? Distillers Grains Quarterly 1(1):15-17.

SAS. 1990. SAS User's Guide: Statistics. Ver. 6a. Cary, N.C.: SAS Institute, Inc.

Spiehs M. J., M. H. Whitney, and G. C. Shurson. 2002. Nutrient database for distiller's dried grain with solubles produced from new ethanol plants in Minnesota and South Dakota. Journal of Animal Science 80:2639-2645.

Stoward, P. J. 1967. The histochemical properties of some periodate- reactive mucosubstances of a pregnant Syrian hamster before and after methylation with methalonic thionyl chloride. Journal of the Royal Microscopical Society 87: 77.

Subramaniam, P. J, O. C. Burke, J. U. Kristott, K. H. M. Groves, and S. A. Jones. Heat Resistant Chocolate; Research Report No. 710 Surrey, UK: Leatherhead Food International, Ltd.

Teunou, E., J. J. Fitzpatrick, and E. C. Synnott. 1999. Characterization of food powders flowability. Journal of Food Engineering 39(1):31-37.

Weigert, K. 1904. Eine Kliene Verbesserung der Hamatoxylin van-Gieson-methode. Zeitschrift für wissenschaftliche Mikroskopie und für mikroskopische.

USDOE (United States Department of Energy). 2007. Fossil Fuels. http:// www.energy.gov. http:// www.energy.gov/energysources/fossilfuels.htm. Accessed on 16 January 2008.

Xiong, Y., Bartle, J. L., and Preston, R. L. 1990. Improved enzymatic method to measure processing effects and starch availability in sorghum grain. J. Anim. Sci. 63:3861.

Table1. Proximate analysis (% db) of the DDGS samples from commercial ethanol plants used in this study. Values in parenthesis are ± 1 standard deviation.*

Plant	Batch	Crude Protein	Crude Fat	Crude Fiber	NDF	ADF	Total starch	Ash
1	1	29.45[1] (0.35)	13.4[1] (0.64)	9.63[1] (0.07)	33.74[1] (1.2)	16.91[2] (1.16)	9.76[1] (0.19)	12.54[1] (1.02)
1	2	29.45[1] (0.07)	10.4[2] (0.0)	10.22[2] (1.46)	29.95 (2.75)	14.08[1] (3.59)	14.00[2] (0.35)	14.00[1] (1.02)
Plant mean		**28.33[b] (1.25)**	**10.76[a] (1.00)**	**9.93[a] (1.45)**	**31.84[b] (4.02)**	**15.56[a] (2.29)**	**11.82[a] (1.2)**	**13.27[a] (3.10)**
2	1	29.85[1] (0.07)	9.15[1] (2.47)	9.52[1] (0.67)	40.02[1] (3.81)	18.25[2] (2.29)	10.4[2] (0.44)	13.41[2] (1.02)
2	2	31.45[2] (0.35)	10.45[2] (0.92)	11.29[2] (1.26)	39.82[1] (1.96)	12.18[1] (1.17)	9.23[1] (0.05)	11.30[1] (1.02)
Plant mean		**30.65[a] (1.20)**	**9.75[a] (1.05)**	**10.30[a] (1.23)**	**39.90[a] (3.95)**	**15.21[a] (3.95)**	**9.81[a] (1.52)**	**12.84[a] (2.56)**
3	1	30.4[1] (0.15)	11.10[1] (0.29)	10.48[1] (0.80)	39.85[2] (2.90)	17.83[1] (1.11)	12.6[2] (0.21)	16.59[2] (1.02)
	2	29.0[1] (0.42)	10.9[1] (0.21)	10.15[1] (1.06)	37.07[1] (1.28)	17.95[1] (2.64)	10.6[1] (0.39)	9.09[1] (1.02)
Plant mean		**28.70[a] (1.32)**	**10.98[a] (0.95)**	**10.32[a] (1.53)**	**38.46[a] (4.01)**	**17.89[a] (4.01)**	**11.59[a] (1.42)**	**11.52[a] (3.05)**
4	1	31.7[2] (0.28)	9.5[1] (0.14)	7.9[1] (0.57)	35.8[1] (0.14)	15.6[1] (0.49)	9.3[2] (0.29)	4.15[2] (0.21)
	2	29.6[1] (0.28)	9.3[1] (0.14)	7.8[1] (0.57)	37.7[1] (0.07)	15.0[1] (0.43)	8.8[1] (0.00)	4.10[1] (0.28)
Plant mean		**30.65[a] (1.23)**	**9.4[b] (0.16)**	**7.85[b] (0.47)**	**36.73[a] (1.07)**	**15.28[a] (0.49)**	**9.05[b] (0.33)**	**4.13[b] (0.21)**
5	1	32.3[1] (0.28)	9.15[1] (0.07)	8.00[1] (0.70)	38.4[1] (0.85)	18.0[2] (0.64)	10.6[2] (0.21)	4.55[1] (0.21)
	2	31.25[1] (0.07)	9.85[1] (0.07)	8.8[1] (1.84)	39.4[2] (0.64)	16.5[1] (1.32)	9.55[1] (0.21)	4.40[1] (0.21)
Plant mean		**31.78[a] (0.63)**	**9.50[b] (0.41)**	**8.40[b] (1.23)**	**38.88[a] (0.86)**	**17.24[a] (1.12)**	**10.05[a] (0.65)**	**4.48[b] (0.22)**

* Same superscript letters indicate there was no significant difference among the plants for a given dependent variable ($p<0.05$, LSD); same superscript numbers indicate there was no significant difference between the batches in a particular plant, for a given dependent variable ($p<0.05$, LSD); n=2 for each plant, each batch.

Table 2. Carbohydrate and protein composition from cross sectional imaging of DDGS particles. Values in parenthesis are ± 1 standard deviation.[†]

Plant	Batch	Mean particle size (mm)	Total area* (mm^2)	Total carbohydrate area (mm^2)	Carbohydrate area (% of cross-section)	Total protein area (mm^2)	Protein area (% of cross-section)
1	1	2.38	4.02 (0.06)	2.00 (0.00)	49.75[1] (0.04)	1.22 (0.00)	30.35[1] (0.02)
		1.68	2.22 (0.00)	0.89 (1.00)	39.93[1] (0.00)	0.93 (0.00)	41.76[1] (0.00)
		1.19	1.01 (0.00)	0.55 (0.00)	53.95[1] (0.30)	0.35 (0.80)	34.27[1] (0.00)
		0.84	0.53 (0.00)	0.31 (0.89)	58.96[1] (0.03)	0.12 (0.72)	22.84[1] (0.23)
	2	2.38	5.33 (0.10)	1.94 (0.06)	36.36[2] (0.00)	1.23 (0.03)	23.15[2] (0.00)
		1.68	2.38 (0.00)	0.93 (0.13)	39.24[1] (0.09)	0.93 (0.07)	39.03[1] (0.00)
		1.19	1.41 (0.00)	0.42 (0.00)	29.95[2] (0.56)	0.40 (0.00)	27.96[2] (0.00)
		0.84	0.58 (0.40)	0.14 (0.00)	24.77[2] (0.00)	0.09 (0.02)	16.31[2] (0.35)
2	1	2.38	4.45 (1.50)	1.24 (0.00)	27.74[1] (1.23)	1.27 (0.00)	28.52[1] (0.00)
		1.68	2.13 (0.00)	0.53 (0.22)	24.60[1] (0.00)	0.55 (0.00)	25.92[2] (0.01)
		1.19	1.29 (0.45)	0.36 (0.00)	28.15[1] (0.33)	0.47 (0.80)	36.38[1] (0.38)
		0.84	0.57 (0.00)	0.15 (0.56)	26.97[1] (0.12)	0.21 (0.32)	35.76[1] (0.70)
	2	2.38	5.32 (0.80)	1.26 (0.00)	23.62[2] (0.00)	0.80 (0.03)	15.14[2] (0.04)
		1.68	2.45 (0.00)	0.73 (0.00)	29.93[2] (1.23)	0.76 (1.01)	30.77[1] (0.01)
		1.19	1.36 (2.30)	0.45 (0.00)	33.52[1] (0.04)	0.36 (0.00)	26.19[2] (0.06)
		0.84	0.81 (0.00)	0.23 (0.15)	27.68 (0.00)	0.32 (0.20)	39.22[1] (0.00)
3	1	2.38	5.55 (0.40)	2.27 (0.00)	40.85[1] (0.00)	1.53 (0.17)	27.51[1] (0.64)
		1.68	2.14 (0.00)	0.65 (0.00)	30.22[1] (0.00)	0.54 (0.00)	25.30[1] (0.01)
		1.19	1.05 (0.67)	0.24 (0.32)	22.64[2] (0.00)	0.24 (0.42)	23.28[2] (0.00)
		0.84	0.53 (0.00)	0.15 (0.60)	29.39[1] (0.01)	0.14 (0.00)	27.11[1] (0.03)
	2	2.38	5.09 (0.05)	1.41 (0.00)	27.69[2] (0.33)	0.84 (0.00)	16.50[2] (0.00)
		1.68	3.21 (0.00)	0.93 (0.00)	29.09[1] (0.01)	0.95 (1.00)	29.72[1] (1.03)
		1.19	1.18 (0.00)	0.36 (0.00)	30.45[1] (0.02)	0.35 (0.07)	29.71[1] (0.01)
		0.84	0.46 (0.75)	0.13 (0.03)	28.30[1] (0.01)	0.12 (0.00)	26.50[1] (0.01)
4	1	2.38	4.14 (0.54)	0.94 (0.00)	22.84[1] (0.01)	0.95 (0.00)	22.96[1] (0.01)
		1.68	2.19 (0.00)	0.64 (0.00)	29.45[1] (0.05)	0.54 (0.50)	24.68[1] (0.51)
		1.19	1.85 (0.00)	0.54 (1.00)	29.38[1] (0.00)	0.56 (0.00)	30.45[1] (0.40)

		0.84	0.55 (0.70)	0.15 (0.49)	26.35[2] (1.40)	0.15 (0.00)	27.25[2] (0.36)
	2	2.38	4.45 (0.02)	1.10 (0.00)	24.82[1] (0.05)	0.97 (0.00)	21.80[1] (1.00)
		1.68	2.04 (0.00)	0.46 (0.51)	22.32[2] (0.47)	0.54 (0.00)	26.63[1] (0.00)
		1.19	1.03 (0.30)	0.15 (0.00)	14.97[2] (0.01)	0.31 (0.39)	30.69[1] (0.02)
		0.84	0.84 (0.00)	0.27 (0.45)	32.02[2] (0.01)	0.31 (0.00)	36.74[1] (0.07)
5	1	2.38	4.33 (0.00)	1.24 (0.00)	28.72[1] (0.20)	1.25 (0.40)	28.92[1] (0.00)
		1.68	3.06 (0.15)	0.97 (0.00)	31.65[2] (0.25)	0.71 (0.71)	23.35[2] (0.00)
		1.19	1.00 (0.39)	0.35 (0.00)	34.38[1] (0.30)	0.35 (0.00)	34.59[1] (0.33)
		0.84	0.67 (0.00)	0.23 (0.41)	34.82[2] (0.00)	0.16 (0.00)	23.11[2] (0.00)
	2	2.38	5.38 (0.02)	1.46 (0.00)	27.23[1] (0.00)	1.66 (0.89)	30.82[1] (0.80)
		1.68	3.04 (0.51)	1.20 (0.00)	39.58[1] (0.06)	1.14 (0.00)	37.58[1] (0.01)
		1.19	1.00 (0.00)	0.22 (0.00)	21.46[1] (0.83)	0.33 (0.02)	33.13[1] (2.30)
		0.84	0.79 (0.00)	0.23 (0.08)	29.73[1] (0.00)	0.21 (0.00)	27.14[1] (0.18)

* Total area represents cross-sectional area of the DDGS particles which was obtained by imaging.

† Similar superscript numbers indicates that there were no significant differences for a particular particle size between batches of a particular plant for that property ($p<0.05$, LSD); n=3 for each sieve size/plant/batch.

Table 3. Mean carbohydrate and protein composition from cross sectional imaging of DDGS particles. Values in parenthesis are ± 1 standard deviation.[x†]

Plant	Mean particle size (mm)	Total area* (mm^2)	Total carbohydrate area (mm^2)	Carbohydrate area (% of cross-section)	Total protein area (mm^2)	Protein area (% of cross-section)
1	2.38	4.67 (0.72)	1.97 (0.03)	43.06[a] (7.33)	1.23 (0.01)	26.75[a] (3.95)
	1.68	2.30 (0.08)	0.91 (0.02)	39.59[a] (0.38)	0.93 (0.00)	40.39[a] (1.50)
	1.19	1.21 (0.22)	0.48 (0.07)	41.95[a] (13.14)	0.37 (0.03)	31.12[a] (3.45)
	0.84	0.55 (0.03)	0.23 (0.09)	41.86[a] (18.72)	0.11 (0.01)	19.57[c] (3.58)
2	2.38	4.88 (0.47)	1.25 (0.01)	25.68[b] (2.26)	1.04 (0.25)	21.83[a] (7.33)
	1.68	2.29 (0.17)	0.63 (0.11)	27.16[b] (2.82)	0.66 (0.11)	28.34[ab] (2.65)
	1.19	1.32 (0.04)	0.41 (0.05)	30.83[a] (2.94)	0.41 (0.06)	31.28[a] (5.58)
	0.84	0.69 (0.13)	0.19 (0.04)	27.32[a] (0.39)	0.26 (0.06)	37.49[a] (1.95)
3	2.38	5.32 (0.25)	1.84 (0.47)	34.27[ab] (7.21)	1.18 (0.38)	22.00[a] (6.03)
	1.68	2.67 (0.59)	0.79 (0.16)	29.66[b] (0.62)	0.75 (0.23)	27.51[bc] (2.42)
	1.19	1.11 (0.07)	0.30 (0.07)	26.55[a] (4.28)	0.30 (0.06)	26.49[a] (3.52)
	0.84	0.50 (0.03)	0.14 (0.01)	28.85[a] (0.60)	0.13 (0.01)	26.80[bc] (0.34)
4	2.38	4.29 (0.17)	1.02 (0.09)	23.83[a] (1.08)	2.96 (0.01)	22.38[a] (0.64)
	1.68	2.12 (0.08)	0.55 (0.10)	25.88[b] (3.91)	0.54 (0.00)	25.65[ab] (1.07)
	1.19	1.44 (0.45)	0.35 (0.21)	22.17[a] (7.89)	0.44 (0.14)	30.57[a] (0.13)
	0.84	0.70 (0.16)	0.21 (0.07)	29.19[a] (3.11)	0.23 (0.09)	32.00[ab] (5.19)
5	2.38	4.86 (0.57)	1.35 (0.12)	27.98[a] (0.82)	1.46 (0.22)	29.87[a] (1.04)
	1.68	3.05 (0.01)	1.09 (0.13)	35.62[ab] (4.35)	0.93 (0.23)	30.47[a] (7.99)
	1.19	1.00 (0.00)	0.28 (0.07)	27.92[a] (7.08)	0.34 (0.02)	33.86[a] (1.66)
	0.84	0.73 (0.06)	0.23 (0.00)	32.27[a] (2.79)	0.18 (0.03)	25.13[bc] (2.20)
		Overall mean for each mean particle size (n=30 for each sieve pore size)[x]				
	2.38	4.81 (0.56)	1.49 (0.92)	30.96[1] (8.37)	1.17 (0.27)	24.56[3] (5.40)
	1.68	2.49 (0.43)	0.79 (0.22)	31.58[2] (5.96)	0.76 (0.21)	30.47[2] (6.42)
	1.19	1.22 (0.26)	0.36 (0.13)	29.88[3] (9.98)	0.37 (0.09)	30.67[1] (3.98)
	0.84	0.63 (0.13)	0.20 (0.06)	31.90[1] (9.59)	0.18 (0.08)	28.20[4] (6.85)

* Total area represents the cross-sectional area of DDGS particles which was obtained by imaging

† Similar superscript letters indicates that there were no significant differences among the plants for a particular particle size for that property ($p<0.05$, LSD); n=3 for each sieve size/plant/batch; thus n=6 for each sieve size/plant.

X Similar superscript numbers indicates there were no significant differences between the particle size for all DDGS samples for that property ($p<0.05$, LSD) ; n=3 for each sieve size/plant/batch; thus n=6 for each sieve size/plant.

Table 4. Physical properties of the DDGS samples from commercial ethanol plants used in this study. Values in parenthesis are ± 1 standard deviation.*

Plant	Batch	Geometric mean diameter (d_{gw}, mm)	Geometric standard deviation (S_{gw}, mm)	Moisture content (%, db)	Soluble level (%, db)
1	1	0.83[1]	0.48[1]	4.32[1] (0.65)	12.56[1] (3.06)
	2	0.87[1]	0.55[1]	4.92[1] (1.03)	12.77[1] (2.12)
Plant mean		**0.80[ab] (0.03)**	**0.52[a] (0.05)**	**4.61[b] (0.87)**	**12.56[ab] (3.06)**
2	1	0.79[1]	0.45[1]	4.60[1] (0.88)	11.03[1] (1.82)
	2	0.21[2]	0.30[1]	5.36[1] (1.25)	13.73[1] (2.59)
Plant mean		**0.50[b] (0.41)**	**0.38[a] (0.12)**	**4.98[b] (1.10)**	**12.34[b] (2.55)**
3	1	1.00[1]	0.45[1]	5.84[1] (1.32)	10.58[1] (1.29)
	2	1.38[2]	0.49[1]	5.38[2] (1.66)	13.38[1] (1.16)
Plant mean		**1.19[a] (0.27)**	**0.47[a] (0.03)**	**5.61[b] (1.44)**	**11.98[b] (1.88)**
4	1	0.80[1]	0.20[1]	6.42[1] (0.35)	14.80[1] (2.82)
	2	0.81[1]	0.53[1]	8.83[1] (2.54)	14.32[1] (2.55)
Plant mean		**0.81[ab] (0.01)**	**0.37[a] (0.23)**	**7.63[a] (2.13)**	**14.59[a] (2.55)**
5	1	0.68[1]	0.47[1]	7.26[1] (0.433)	12.26[1] (1.82)
	2	0.97[2]	0.54[1]	8.89[1] (3.18)	11.26[1] (1.40)
Plant mean		**0.83[ab] (0.21)**	**0.51[a] (0.05)**	**8.08[a] (2.31)**	**11.41[b] (1.54)**

* Same superscript letters indicate there was no significant difference among the plants for a given dependent variable ($p<0.05$, LSD); same superscript numbers indicate there was no significant difference between the batches in a particular plant, for a given dependent variable ($p<0.05$, LSD); n=5 for each plant, each batch.

Table 5. Some key flowability parameters for the DDGS samples used in this study were determined by Bhadra et al. (2007). Values in parenthesis are ±1 standard deviation.*

Plant	Batch	Angle of Repose (^{o})	Hausner Ratio$^\beta$ (-)	Total Flowability Index (-)	Total Floodability Index (-)	Flow Function Index$^\gamma$ (-)	
						Level 1$^\delta$ Consolidation	Level 2$^\delta$ Consolidation
1	1	35.94^2 (1.37)	1.09^1 (0.03)	81.40^1 (0.89)	63.60^1 (3.78)	4.56^2 (2.12)	2.25^2 (1.39)
	2	40.62^1 (0.34)	1.08^1 (0.00)	81.00^1 (0.00)	63.41^1 (3.13)	5.35^1 (0.23)	2.47^1 (0.56)
Batch mean		**38.28^b (2.64)**	**1.08^b (0.02)**	**81.20^a (0.63)**	**63.50^a (3.27)**	**4.96^b (0.56)**	**2.36^c (0.16)**
2	1	37.76^2 (0.74)	1.04^1 (0.04)	82.40^1 (0.96)	53.52^2 (0.64)	1.43^2 (0.25)	1.45^1 (0.69)
	2	41.60^1 (1.41)	1.03^1 (0.01)	80.80^2 (0.84)	57.47^1 (1.84)	1.79^1 (1.10)	1.59^1 (1.17)
Batch mean		**39.68^a (2.22)**	**1.04^a (0.02)**	**81.60^a (1.20)**	**55.35^b (2.57)**	**1.61^e (0.25)**	**1.52^e (0.10)**
3	1	39.48^2 (0.64)	1.04^1 (0.01)	80.80^2 (0.84)	70.20^1 (0.45)	5.57^1 (0.25)	5.69^1 (0.38)
	2	40.76^1 (0.85)	1.04^1 (0.02)	82.10^1 (1.14)	60.70^1 (2.41)	4.55^2 (1.01)	4.83^2 (1.30)
Batch mean		**40.12^a (0.98)**	**1.04^a (0.01)**	**81.45^a (1.17)**	**65.27^a (5.27)**	**5.06^a (0.72)**	**5.26^a (0.61)**
4	1	37.26^1 (1.04)	1.03^1 (0.01)	82.00^1 (0.71)	70.20^1 (1.15)	3.47^1 (0.01)	2.53^2 (0.7)
	2	38.98^1 (1.28)	1.08^2 (0.01)	79.40^2 (1.29)	62.10^1 (0.65)	3.27^1 (2.14)	4.37^1 (1.7)
Batch mean		**38.12^b (1.43)**	**1.06^a (0.03)**	**80.70^{ab} (1.69)**	**66.15^a (4.36)**	**3.37^{cd} (0.14)**	**3.45^b (1.30)**
5	1	39.82^1 (1.41)	1.05^1 (0.01)	79.20^1 (0.76)	48.60^2 (1.52)	3.28^1 (0.17)	2.18^1 (0.10)
	2	38.722 (1.04)	1.06^1 (0.01)	79.30^1 (0.45)	64.60^1 (1.52)	3.07^2 (0.14)	1.90^2 (0.25)
Batch mean		**39.27^{ab} (1.31)**	**1.05^a (0.01)**	**79.55^b (0.64)**	**56.85^b (8.55)**	**3.18^d (0.15)**	**2.04^d (0.20)**

* Same superscript number indicates that there was no significant difference among batches for a particular plant for that property ($p<0.05$, LSD);same superscript letters indicates that there was no significant difference among the plants for that property ($p<0.05$, LSD); n=5 for each plant/batch unless noted otherwise

β Hausner ratio is defined as ratio of packed bulk density to aerated bulk density

γ n=3 for each plant/batch for this property

δ Level one consolidation means it had 14.5 kg used as the consolidation weight per the Jenike (1964) shear testing procedure, as discussed in Bhadra et al. (2007); Level two consolidation means it had 3 kg used as the consolidation weight per the Jenike (1964) shear testing procedure as discussed in Bhadra et al. (2007)

Table 6. Surface thickness of carbohydrate and protein components on DDGS particles. Values in parenthesis are ±1 standard deviation.*

			Carbohydrate		Protein	
Plant	**Batch**	**Diameter (mm)**	**Maximum Thickness (μm)**	**Minimum Thickness (μm)**	**Maximum Thickness (μm)**	**Minimum Thickness (μm)**
1	1	2.28	3.00	0.25	3.21	1.92
	2		2.56	0.70	2.57	0.53
Plant mean			**2.78^{a} (0.31)**	**0.48^{b} (0.32)**	**2.56^{b} (0.86)**	**1.23^{b} (0.98)**
2	1	2.28	0.65	0.12	0.11	0.00
	2		0.59	0.20	0.75	0.23
Plant mean			**0.62^{e} (0.04)**	**0.16^{e} (0.06)**	**0.75^{d} (2.56)**	**0.12^{c} (0.16)**
3	1	2.28	4.80	2.00	0.57	0.11
	2		0.40	0.20	1.27	0.23
Plant mean			**2.60^{bc} (3.11)**	**1.09^{d} (1.28)**	**1.27^{c} (2.56)**	**0.23^{d} (0.17)**
4	1	2.28	2.50	0.35	3.79	2.53
	2		0.75	0.21	2.57	0.52
Plant mean			**2.63^{bc} (2.65)**	**0.28^{c} (0.10)**	**2.57^{ab} (2.56)**	**1.53^{a} (1.42)**
5	1	2.28	1.25	0.45	0.80	0.35
	2		1.70	0.75	1.21	0.45
Plant mean			**1.48^{d} (0.32)**	**0.60^{a} (0.21)**	**2.56^{b} (0.29)**	**0.40^{c} (0.07)**

* Similar superscript letters indicates that there were no significant differences among the plants for that property ($p<0.05$, LSD); n=1 for each plant/batch

Table 7. Flow function classification according to the Jenike (1964) shear testing methodology.

Flow functions	Classification of flow
F<1	No flow
1<F<2	Highly cohesive
2<F<4	Cohesive
4<F<10	Intermittent flow
10<F	Free flow

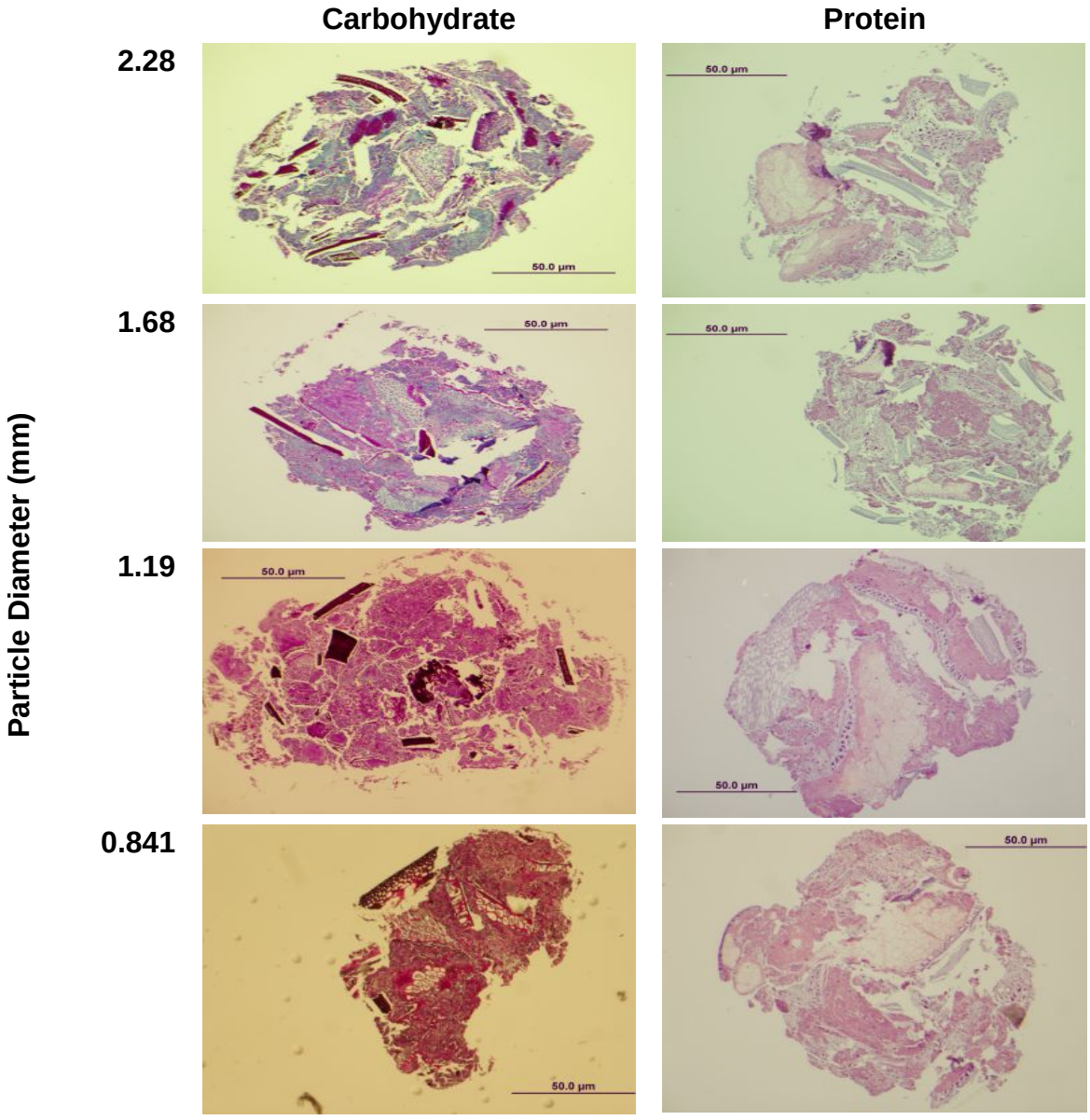

Figure 1. **Representative carbohydrate and protein cross-section images for DDGS particles. Carbohydrate is denoted by dark purple, and protein by pink color. (These particles were from Plant 1, Batch 1.)**

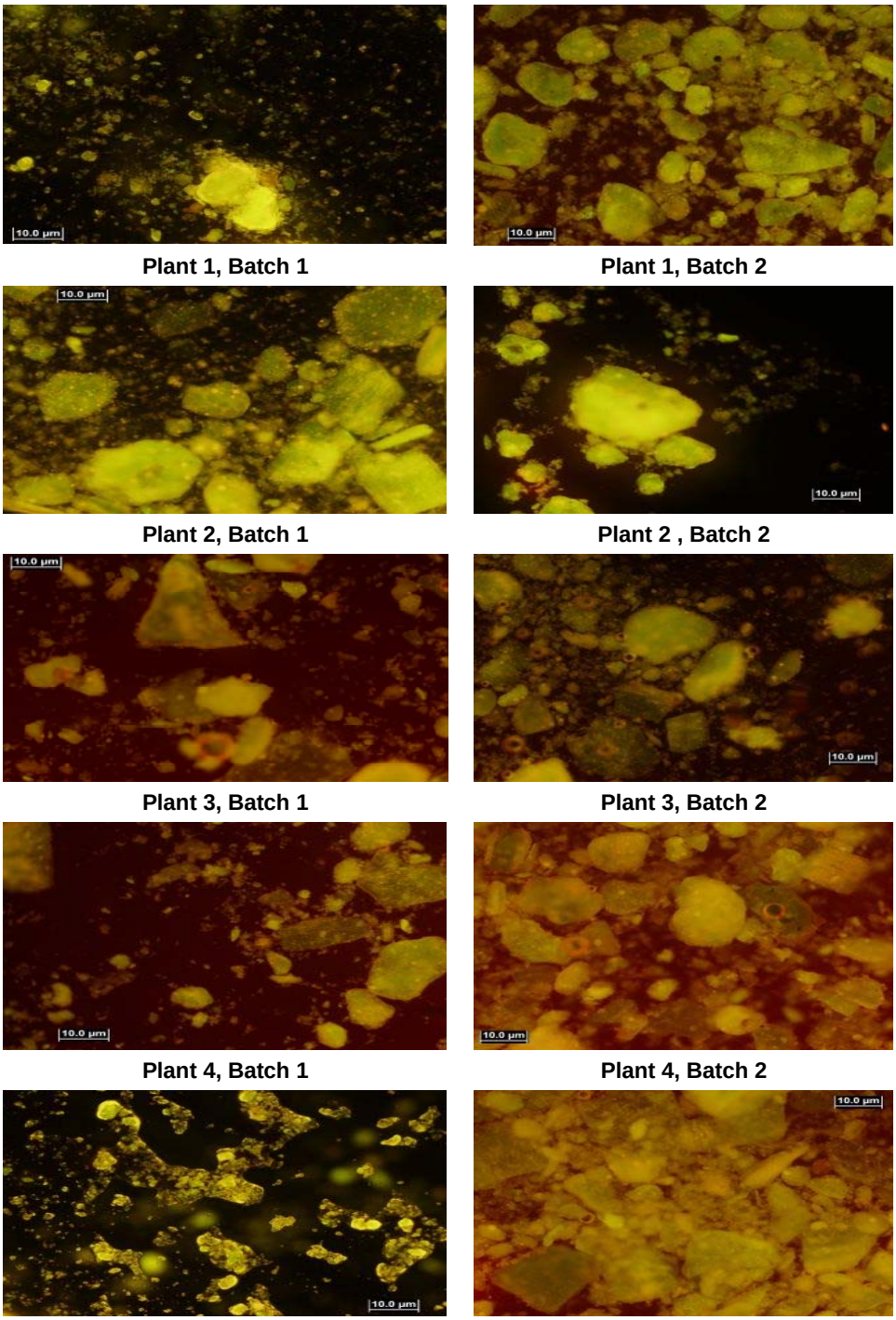

Figure 2. Representative surface fat images of DDGS particles at 10X magnification. (These particles were from a sieve diameter of 0.074 mm.)

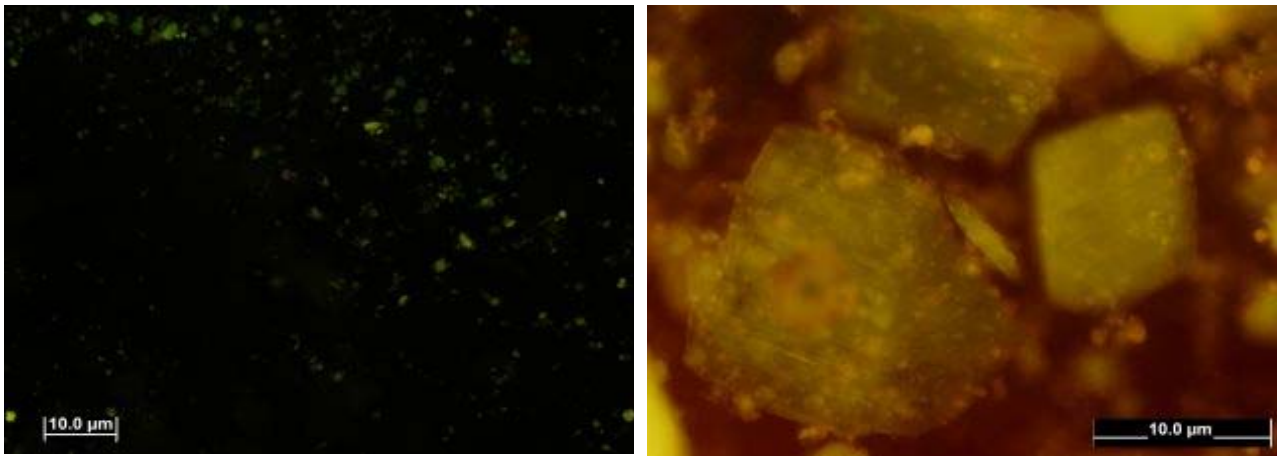

a b

Figure 3. a) Surface fat images for control DDGS (without fat stain) at 10X magnification; b) Surface fat images at 40 X magnification for DDGS (from plant 5, batch 2) using fat stain.